JPE 15-4-21

http://dx.doi.org/10.6113/JPE.2015.15.4.1074
ISSN(Print): 1598-2092 / ISSN(Online): 2093-4718

A Novel AC Solid-State Circuit Breaker with Reclosing and Rebreaking Capability

Jin-Young Kim*, Seung-Soo Choi*, and In-Dong Kim†

*†Department of Electrical Engineering, Pukyong National University, Busan, Korea

Abstract

These days, the widespread use of sensitive loads and distributed generators makes the solid-state circuit breaker (SSCB) an essential component in power circuits to achieve a high power quality for AC Grids. In traditional AC SSCB using SCRs, some auxiliary mechanical devices are required to make the reclosing operation possible before fault recovery. However, the proposed AC SSCB can break quickly and then be reclosed without auxiliary mechanical devices even during the short-circuit fault. Moreover, its fault current breaking time is short and its SSCB reclosing operation is fast. This results in a reduction of the economic losses due to fault currents and power outages. Through simulations and experiments on short-circuit faults, the performance characteristics of the proposed AC SSCB are verified. A design guideline is also suggested to apply the proposed AC SSCB to various AC grids.

Key words: AC SSCB, Operating duty, Rebreaking capability, Reclosing operation, Solid-state circuit breaker (SSCB), Thyristor

I. INTRODUCTION

With the development of the IT industry, a lot of loads that are sensitive to power quality problems are being widely utilized [1]. Furthermore, because of the tendency to widely utilize distributed generators that are sensitive to natural phenomena such as strong winds, lightning, and heavy snow, more reliable and stable power supply technologies are needed [2], [3].

Power grid breakdowns occur frequently due to unwanted contact between power lines and the surrounding environment. If a quick break of fault current is not performed, serious damages may occur due to a rapid increase in the fault current and its resulting electrical fires [4]. Even durring the short-duration faults caused by strong wind or trees, the power grid should be able to supply utility power to loads through quick fault recovery from the initial fault breaking operation. After an initial fault breaking operation, a long-duration sustained interruption without fault recovery may result in a lot of serious economic losses [5].

For this reason, IEEE std C37.09 prescribes a circuit breaker's reclosing and rebreaking operations should be able to be performed repeatedly [6].

In order to ensure a good power quality for the AC power grid, the technology of a circuit breaker must identify a voltage sag/swell, overcurrent, or short circuit fault, and then immediately interrupt it. Furthermore, the circuit breaker should be able to perform a rapid reclosing operation even under a short circuit of the load side, and interrupt the fault.

Power devices for breaking grid faults include the mechanical breaker and the SSCB (Solid-State Circuit Breaker). The mechanical breaker is capable of interrupting faults in several tens [ms] due to its physical structure, which results in a slow interruption capability. Thus, it is difficult to prevent damage to sensitive loads [7].

In contrast, the SSCB can interrupt faults within 4 [ms] in a much lower current level than the allowable peak fault current level so that it can reduce the damage to grid devices [8]. There are several types of semiconductor switching elements used to implement the SSCB such as IGBTs, GCTs, SCRs, and GTOs. Although the SCR requires a commutation circuit for turn-off, it is highly suitable for use in AC SSCB because it is economical and its on-state loss is relatively small [9].

Fig. 1 shows an existing AC SSCB circuit using a SCR that can break the fault current of a single-phase AC circuit [10]. In the circuit of Fig. 1, AC power is supplied through the main SCRs, T_{main1} and T_{main2}. When a fault occurs, the fault

Manuscript received Dec. 12, 2014; accepted Mar. 30, 2015
Recommended for publication by Associate Editor Kyo-Beum Lee.
†Corresponding Author: idkim@pknu.ac.kr
Tel: +82-51-629-6318, Fax: +82-51-629-6305, Pukyong Nat'l Univ.
*Dept. of Electrical Engineering, Pukyong National University, Korea

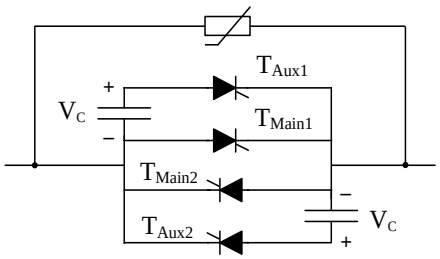

Fig. 1. Previous basic forced commutation circuit.

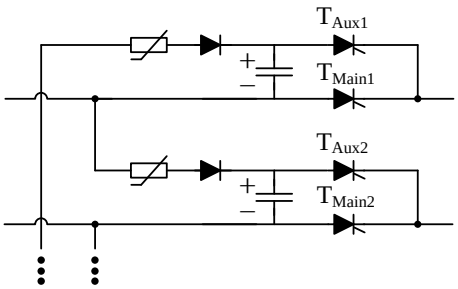

Fig. 2. Previous varistor charging circuit.

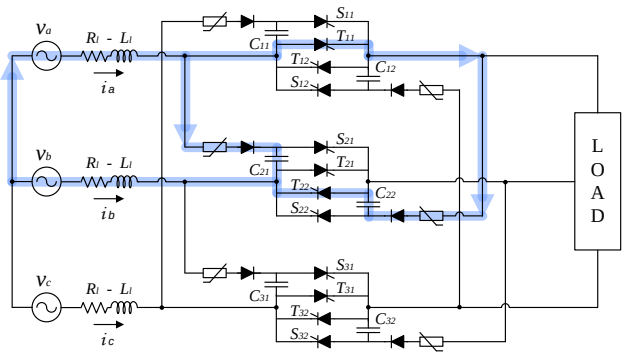

Fig. 3. Previous three-phase SSCB and charging loop of C_{21}, C_{22}.

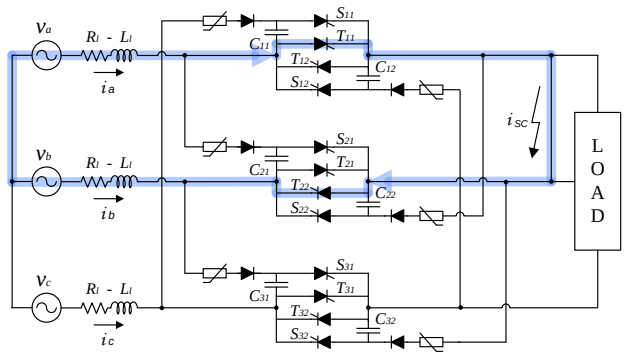

Fig. 4. Charging loop when short fault occurs in Fig. 3.

current can be broken immediately as the auxiliary SCR, T_{aux1} or T_{aux2} is turned on depending on the direction of the current. However, as shown in Fig. 1, in order to turn off the main SCR, the commutation capacitor must be charged in advance.

Fig. 2 shows a circuit for charging the commutation capacitor of Fig. 1 [10]. It is possible to charge the commutation capacitor to a required voltage by using the line voltage and varistor.

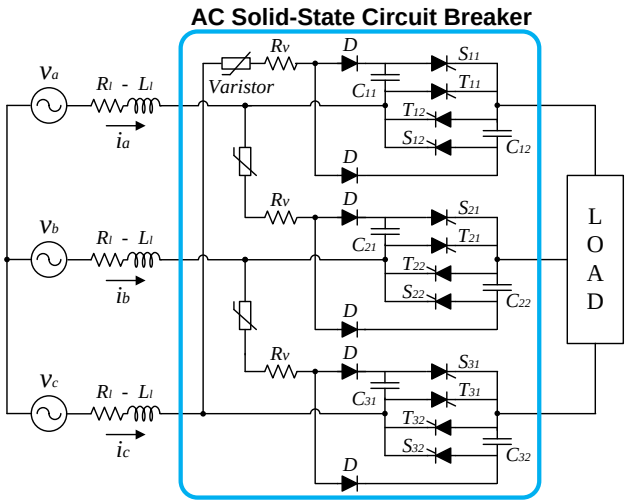

Fig. 5. Proposed AC Solid-State Circuit Breaker(AC SSCB).

Fig. 3 shows a previous three-phase SSCB using the circuits of Fig. 1 and Fig. 2 [10]. The thick line of Fig. 3 shows the loop where the capacitors C_{21} and C_{22} on the b-phase are charged by the line voltage V_{ab}. In the circuit of Fig. 3, when a short circuit fault occurs, the previous three-phase SSCB may break rapidly because it has the same breaking principle as shown in Fig. 1. However, the circuit of Fig. 3 has a significant disadvantage since it is unable to perform the reclosing and rebreaking operations. If explained in further detail, if a short circuit faults lasts on the load side, as shown in Fig. 4, the capacitors C_{21} and C_{22} may not be charged even if the SCRs, T_{11} and T_{22} are turned on, which makes it impossible to reclose and rebreak the previous AC SSCB of Fig. 3.

To overcome such shortcomings, this paper proposes a new AC SSCB that has quick reclosing and rebreaking capabilities. Thus, it can perform the operating duties of reclosing and rebreaking regardless of the circuit state on the load side. In addition, this paper suggests design guidelines in order to apply this AC SSCB to systems of different capacities and applications regardless of the ground system. The proposed AC SSCB is designed and implemented in a rated power of 5 [kW] and a line voltage of 220 [V]. Thus, the operating characteristics are confirmed by simulation and experimental results.

II. Proposed AC Solid-State Circuit Breaker

Fig. 5 shows the proposed AC SSCB circuit. Even under a short circuit fault on the load side, the proposed SSCB can charge the commutation capacitor. In other words, since the recharging operation of the commutation capacitor is possible regardless of the fault state on the load side, the proposed AC SSCB can perform the operation duties of reclosing and rebreaking as prescribed in the circuit breaker standard [6].

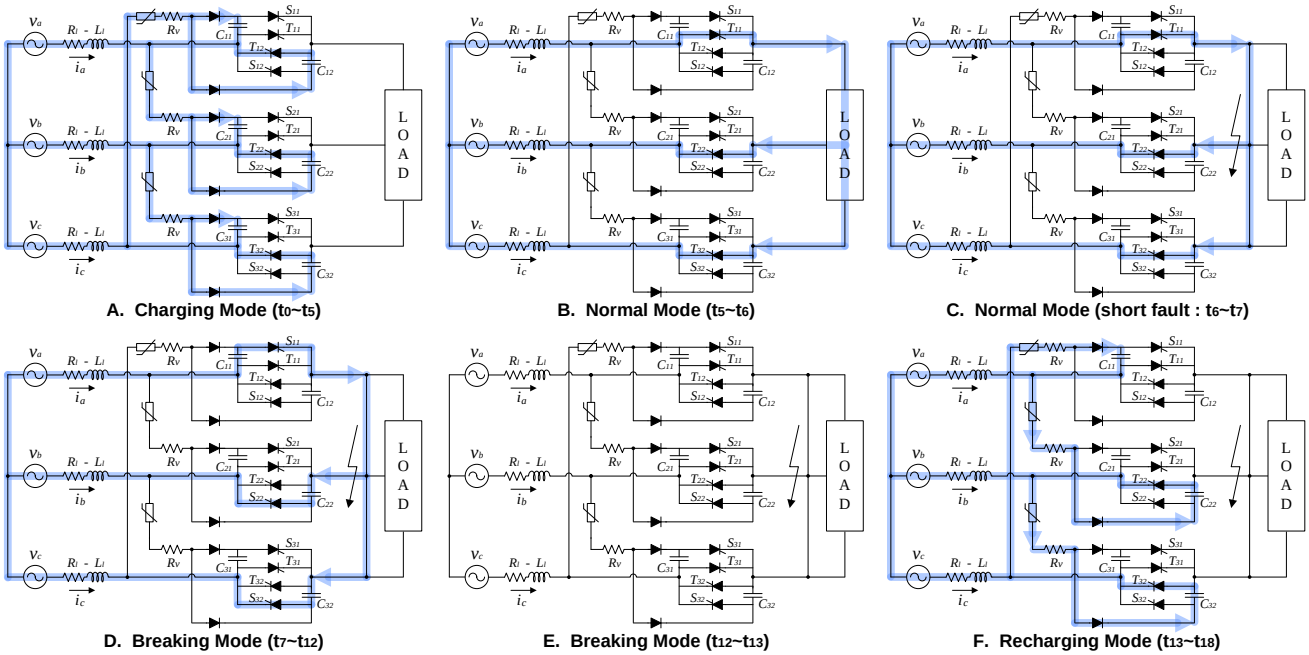

Fig. 6. Operating modes of the proposed AC SSCB.

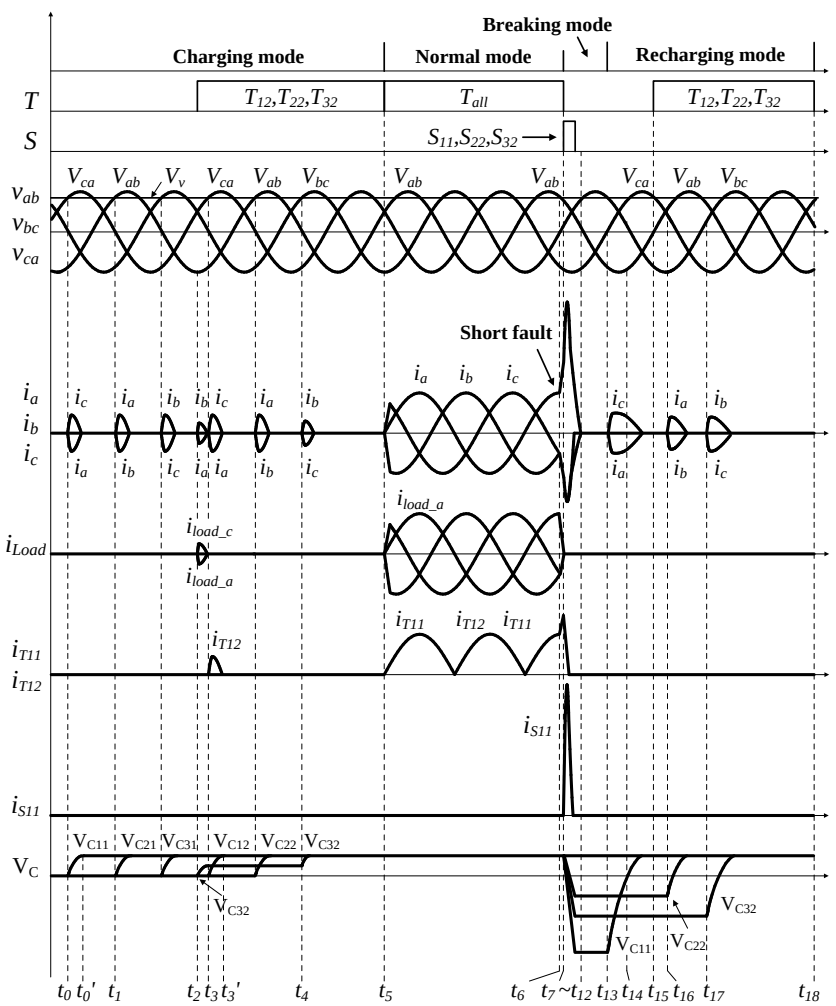

Fig. 7. Operating waveforms of the proposed AC SSCB.

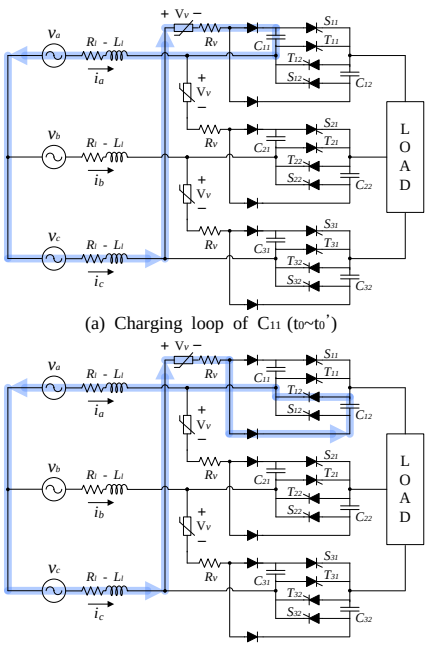

Fig. 8. Charging loop in charging mode

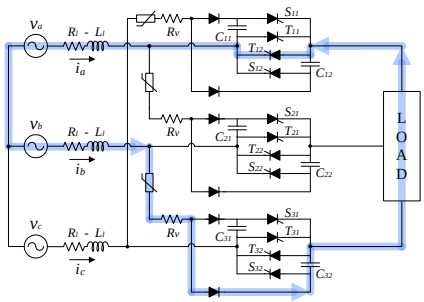

Fig. 9. Charging loop of capacitor C_{32} (t_2~t_3).

The operation of the proposed SSCB may be divided into four modes. The four operation modes are composed of the charging mode, to charge the commutation capacitor; the normal mode, to supply energy to the load; the breaking mode, to break the fault current; and the recharging mode, for reclosing.

In order to confirm the operating characteristics of the proposed SSCB, this paper verifies the breaking and reclosing operations of the SSCB by simulating a three-phase short circuit fault, and as the worst-case, one with the largest fault current value.

Fig. 6 shows the circuit operation according to the modes of the proposed AC SSCB, and Fig. 7 shows the operation waveform corresponding to each mode. The operating characteristics of each mode are as follows.

A. Charging Mode ($t_0 \le t < t_5$)

In the charging mode, all of the commutation capacitors of the AC SSCB must be charged before a faults take place so that the SSCB can interrupt the fault current by using the pre-charged commutation capacitors. Thus, during the charging mode (t_0-t_5) of the SSCB, the commutation capacitor is charged to the voltage level required for breaking by using the line voltage and varistor. The commutation capacitors are divided into two groups; that is, C_{11}, C_{21}, and C_{31} are charged naturally by the line voltages, and C_{12}, C_{22}, and C_{32} are charged through the SCRs.

Fig. 8 shows the loop where the capacitors C_{11} and C_{12} of the a-phase are charged by the line voltage V_{ca}. In the circuit (a) of Fig. 8, the capacitor C_{11} has a charging loop that does not contain the SCR. Therefore, the natural charging (t_0-t_0') is performed when the line voltage V_{ca} is higher than the breakdown voltage V_v of the varistor.

However, the capacitor C_{12} cannot be charged naturally because the charging loop contains the SCR, T_{12} as shown in Fig. 8(b). The capacitor C_{12} can be charged by turning on the SCR, T_{12} at t_3 where the line voltage Vab is higher than the breakdown voltage of the varistor.

By using the charging principle shown in Fig. 8, it is possible to charge all of the capacitors in each phase. However, individually turning on the SCRs, T_{12}, T_{22}, and T_{32} according to the magnitude and phase of the line voltage may require complex control. Thus, as in the charging mode of Fig. 7, it is possible to charge the capacitors C_{12}, C_{22}, and C_{32} together by turning on the SCRs, T_{12}, T_{22}, and T_{32} at the same time during t_1-t_5 (1-3 cycles of the power grid). This enables all of the capacitors to be charged with a simple SCR control.

Of course there may be a charging loop that contains the load, as shown in Fig. 9. The additional charging loop of Fig. 9 does not matter because the magnitude of the charging current is small due to the load impedance. Thus, turning on the SCRs, T_{12}, T_{22}, and T_{32} at the same time can charge all of the capacitors with a simple SCR control.

B. Normal Mode ($t_5 \le t < t_6$)

The normal mode is the steady-state operating mode of the AC SSCB. Since all of the SCRs, T_{all} (T_{11}, T_{12}, T_{21}, T_{22}, T_{31}, and T_{32}) are turned on, energy is supplied to the load as shown in circuit B of Fig. 6. In this mode, such faults as sags/swells of the voltage and over-current are monitored by detecting the line voltages and line currents.

C. Normal Mode (short circuit fault : $t_6 \le t < t_7$)

Mode C is the section where the fault current increases when a three-phase short circuit fault occurs at t_6. Although a short circuit fault has already occurred, the SSCB operates as in the normal mode because the magnitude of the fault current is still smaller than the preset reference current to determine a short circuit fault.

As the a-phase current i_a gradually increases to be equal to the reference value, the AC SSCB starts to break the short circuit fault at t_7. Thus, the breaking mode begins.

D. Breaking Mode ($t_7 \le t < t_{12}$)

The breaking mode is the section where the fault current is interrupted. If the auxiliary SCRs, S_{11}, S_{22}, and S_{32} are turned on, as shown in circuit D of Fig. 6, according to the directions of each phase current, the related main SCRs, T_{11}, T_{22}, and T_{32} are turned off by the pre-charged voltage of the capacitors C_{11}, C_{22}, and C_{32}. As the current through R_l, L_l, and C flows in each phase, the fault current is interrupted. The capacitors C_{11}, C_{22}, or C_{32} discharged for fault current interruption are reversely charged as the waveform V_C of Fig. 7.

E. Breaking Mode ($t_{12} \le t < t_{13}$)

This mode is the section where the fault current is completely broken. Thus, no current flows in the SSCB.

F. Recharging Mode ($t_{13} \le t < t_{18}$)

This recharging mode is the section where the commutation capacitors discharged in the previous breaking mode are recharged again. Figures 10 and 11 show the recharging loops of the capacitors C_{11}, C_{22}, and C_{32} at the recharging mode (t_{13}-t_{18}).

This mode is divided into two time durations. During the first time duration without thyristor triggering signals, the capacitor C_{11} is naturally charged by the line voltage V_{ca}. During the second time duration with thyristor triggering signals, the capacitors C_{22} and C_{32} are recharged through the turned-on SCR, T_{22} and T_{32}. As shown in Figures 10 and 11, if the fault keeps going, the recharging modes are carried out without passing through the load side.

However, if the fault is removed, the recharging loop may also exist through the load side, as shown in Fig. 9, during the second time duration of simultaneously turning on the SCRs, T_{12}, T_{22}, and T_{32} together.

In other words, the proposed SSCB can recharge the

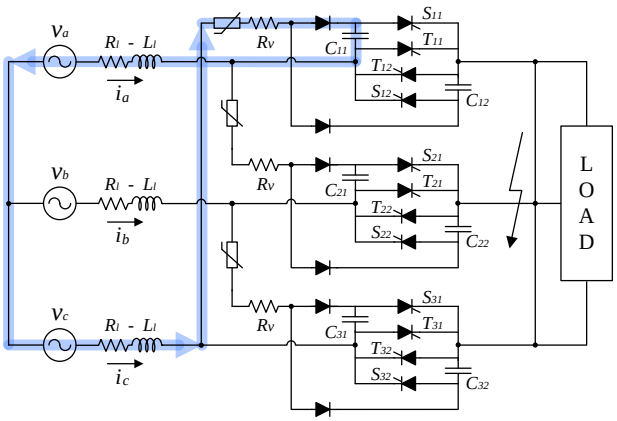

(a) Charging loop of C_{11} ($t_{13} \sim t_{15}$)

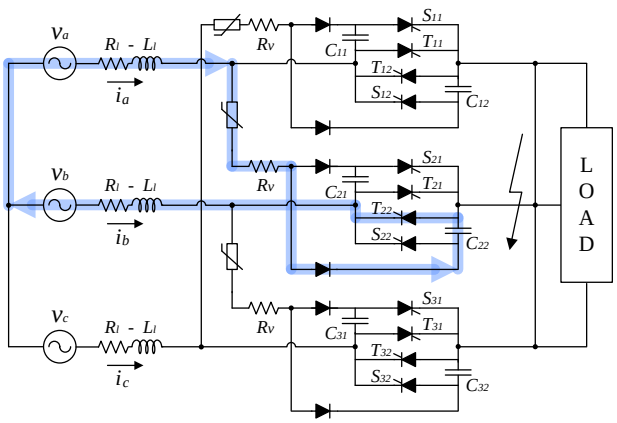

(b) Charging loop of C_{22} ($t_{16} \sim t_{17}$)

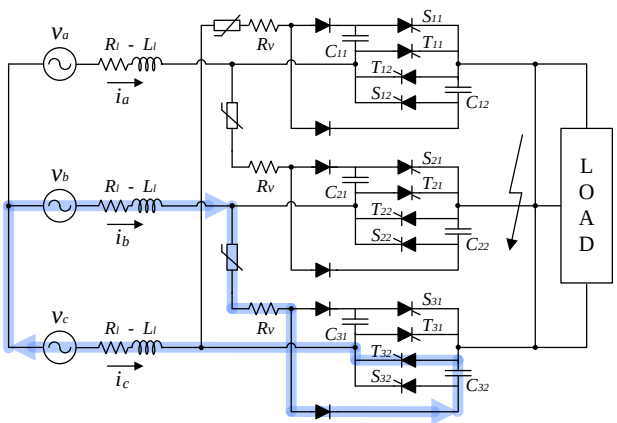

(c) Charging loop of C_{32} ($t_{17} \sim t_{18}$)

Fig. 10. Charging loops of capacitors in recharging mode.

commutation capacitors even under a short circuit on the load side. If the recharging mode is already completed, the SSCB may perform a reclosing operation by turning on the main SCRs because even in the case of a short circuit fault on the load side, the proposed SSCB can rebreak the fault current.

III. Analysis and Design of the Proposed AC SSCB

The design specification and system parameters of the proposed SSCB are shown in Table I. R_v, C, SCR, and the varistor of the SSCB should be selected considering all of the currents through each device and all of the voltages across each device during the charging mode, breaking mode, and recharging mode.

TABLE I
Design Specification and Parameters

Parameters	Specification
Power rating	5 [kW]
Line voltage	220 [V]
Full load current	13.1 [A]
Line resistance R_L	100 [mΩ]
Line inductance L_L	100 [uH] (0.377%)
Short fault switch resistance	100 [mΩ]
Range of trip setting	13.1 [A] → 50 [A]

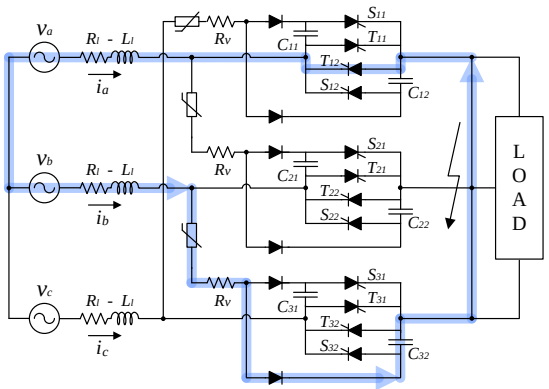

Fig. 11. Additionally possible charging loop of capacitor C_{32} ($t_{14} \sim t_{15}$).

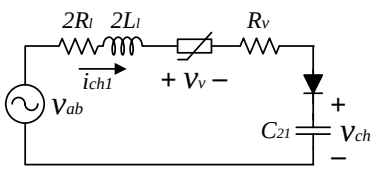

(a) C_{21} charging circuit

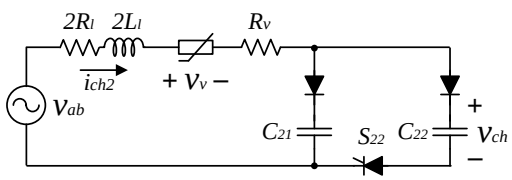

(b) C_{21}, C_{22} charging circuit

Fig. 12. Equivalent circuit of charging mode.

A. Charging Mode ($t_0 \le t < t_5$)

The charging mode is divided into two cases. The first case is where a single capacitor is charged, as shown in Fig. 12(a), and the other case is where two capacitors are charged by turning on the SCR, S_{22}, as shown in Fig. 12(b). The charging current begins to flow when the line voltage V_{ab} is higher than the breakdown voltage V_v of the varistor. The input voltage V_{ab}, the charging currents i_{ch1} and i_{ch2} of the charging circuit, and the charged voltage V_{ch} of the commutation capacitor are expressed as Equations (1), (2), (3), and (4),

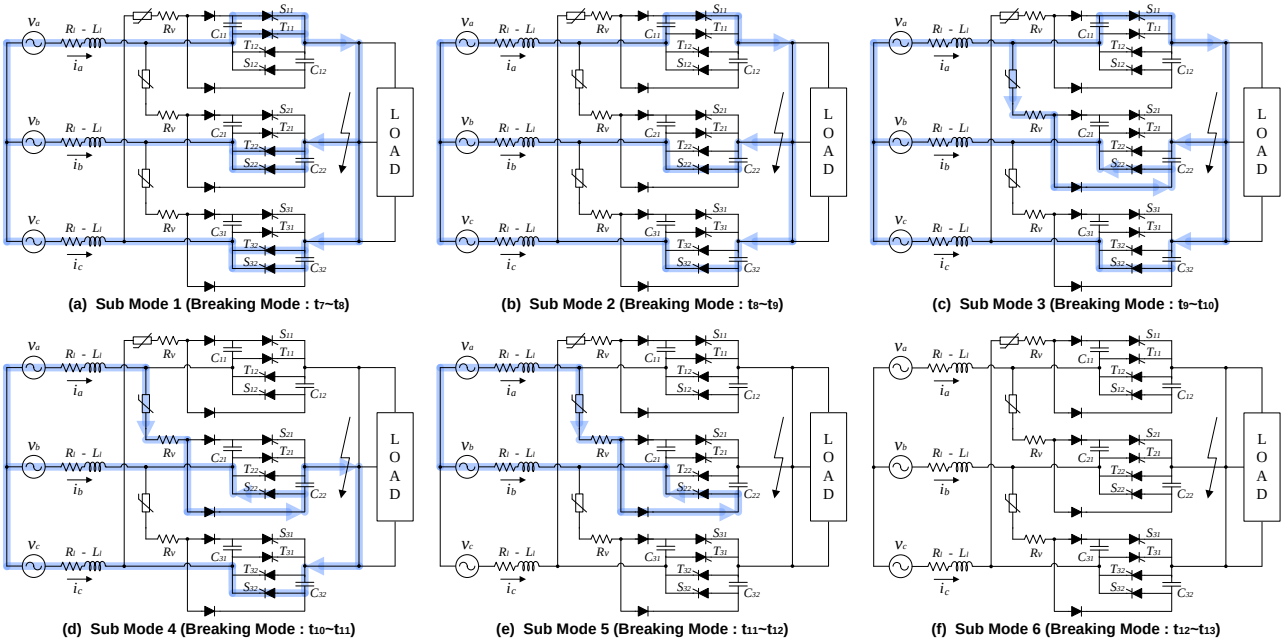

Fig. 13. Detailed sub operating modes of breaking mode.

respectively.

In the charging mode, it should be noted that the commutation capacitor might be charged to a voltage higher than the desired voltage in the case of an underdamped circuit condition. If so, the voltage rating of the commutation capacitor may increase and the peak value of the fault current may increase, resulting in larger SCR capacity. To limit the charged voltage of the commutation capacitor during the charging mode, the resistor R_v should be selected to satisfy the condition of Equation (5). The charging current i_{ch} and charged voltage V_{ch} of the charging mode are lower than those of the other modes. Thus, the capacitor C should be selected earlier than R_V by considering the breaking mode and recharging mode instead of the charging mode.

$$v_{ab}(t) = V_{ab}\sqrt{2}\sin(\omega t + \theta) \quad \left(\theta = \sin^{-1}(\frac{V_v}{V_{ab}\sqrt{2}})\right) \tag{1}$$

$$i_{ch1}(s) = \frac{V_{ab}\sqrt{2}s(\omega\cdot\cos\theta + s\cdot\sin\theta) - V_v(s^2+\omega^2)}{2L_l(s^2+\omega^2)(s^2+\frac{2R_l+R_v}{2L_l}\cdot s+\frac{1}{2L_lC})} \tag{2}$$

$$i_{ch2}(s) = \frac{V_{ab}\sqrt{2}s(\omega\cdot\cos\theta + s\cdot\sin\theta) - V_v(s^2+\omega^2)}{2L_l(s^2+\omega^2)(s^2+\frac{2R_l+R_v}{2L_l}\cdot s+\frac{1}{4L_lC})} \tag{3}$$

$$V_{ch} = V_{ab}\sqrt{2} - V_v \quad [V] \tag{4}$$

$$R_v \geq \sqrt{\frac{8L_l}{C}} - 2R_l \tag{5}$$

B. Charging Mode (short circuit fault: $t_7 \leq t < t_{13}$)

Fig. 13 shows the operation of the SSCB in the breaking mode (t_7-t_{13}) in greater detail.

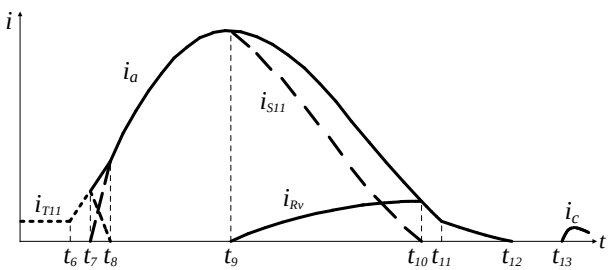

Fig. 14. a-Phase current waveforms in breaking mode.

When a three-phase short circuit fault occurs, the fault current has the largest peak value, which is the worst-case condition. Fig. 14 shows the current waveform through each device on the a-phase for the breaking mode (t_7-t_{12}) in a three-phase short circuit fault.

The components of the AC SSCB should be selected considering the worst-case current flowing through the power devices during the breaking mode operation. To achieve this, it is necessary to know the peak current of the a-phase current i_a of Figs. 13 and 14. In Fig. 14, the a-phase current i_a flows at t_8-t_9 or t_9-t_{10} through the varistor of the breakdown voltage Vv and the capacitor of the capacitance C. Thus, the peak value of the a-phase current i_a is determined by L_l, V_v, and C, as shown in Fig. 15 and Fig. 16.

As the breakdown voltage V_v of the varistor becomes higher, the charged voltage of the capacitor becomes lower by Equation (4). Therefore, as shown in Fig. 16, if the capacitance C and charged voltage V_{ch} become smaller, the peak value of the a-phase current i_a becomes smaller.

However, as the capacitance C of the commutation capacitor and the charged voltage V_{ch} become smaller, the

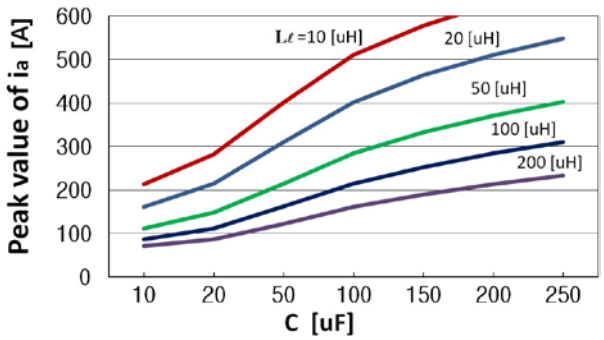

Fig. 15. Peak value of current i_a when C and L_l change.

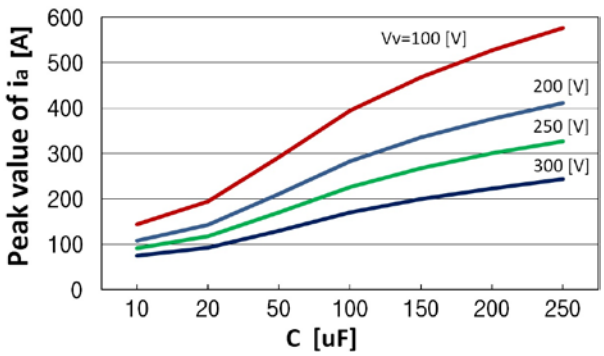

Fig. 16. Peak value of current i_a when C and V_V change.

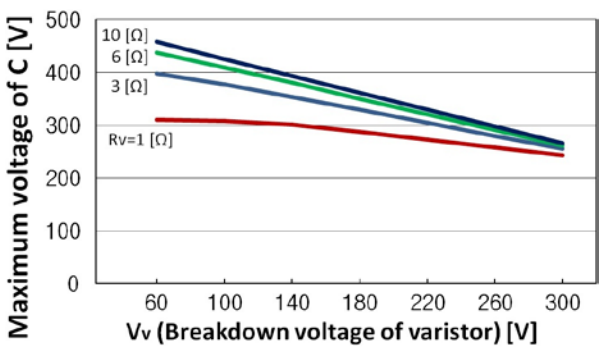

Fig. 17. Maximum voltage of C when V_V and R_V change.

time duration where the commutation capacitor can apply a negative voltage to the turned-off main thyristor becomes shorter. If the time duration is shorter than the turn-off time tq of the main SCRs, the main thyristors might fail to be turned off. Thus, the breakdown voltage V_V of the varistor and the capacitance C of the commutation capacitor should be selected considering the tq of the main SCRs.

The capacitor voltage Vc is reversely charged by the current i_{S11}, as shown in the breaking mode of Fig. 7. At the time instant t_{10} of Fig. 14 the current i_{S11} becomes zero, and the capacitor voltage reaches the maximum value.

As the resistance Rv increases, the current i_{Rv} decreases and the current i_{S11} increases. Thus, the capacitor voltage Vc becomes higher. As a result, the maximum value of the capacitor voltage is determined in accordance with the resistance R_V and the breakdown voltage V_V of the varistor, as shown in Fig. 17.

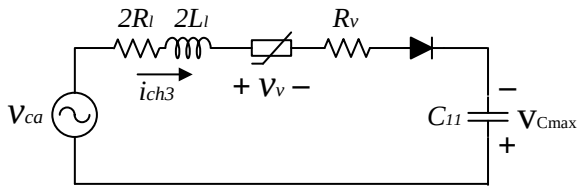

Fig. 18. Equivalent circuit of recharging mode.

C. Recharging Mode ($t_{13} \le t < t_{18}$)

Fig. 18 shows the equivalent circuit of Fig. 10-(a) where the capacitor C_{11} is recharged in the recharging mode. The equivalent circuit of Fig. 11 including the short circuit on the load side is the same as that in Fig. 18. In the recharging mode, the commutation capacitor is charged in the reverse direction unlike the charging mode. At t_{13} of Fig. 7, the line voltage V_{ca} is less than the breakdown voltage V_V of the varistor. However, if Equation (6) is met, the recharging operation of the capacitor begins.

The input voltage V_{ca} of the recharging circuit and the charging current i_{ch} are expressed as Equations (7) and (8), respectively. The final voltage recharged in the capacitor is the same as the result in Equation (4) of the charging mode.

Since the breakdown voltage V_V of the varistor and the capacitor C are properly selected in the breaking mode, the recharging time of the capacitor may be controlled by using the resistor R_v. As the resistance of R_v becomes larger, the recharging time of the capacitor increases and the maximum voltage of the capacitor becomes higher as shown in Fig. 17. Therefore, the resistance of R_v should be selected at the lowest resistance within the operation range to satisfy Equation (5).

$$v_{ca}(t) + V_{C\max} \ge V_v \tag{6}$$

$$v_{ca}(t) = V_{ca}\sqrt{2}\sin(\omega t + \theta_2) \quad \left(\theta_2 = \sin^{-1}\left(\frac{V_v - V_{C\max}}{V_{ca}\sqrt{2}}\right)\right) \tag{7}$$

$$i_{ch3}(s) = \frac{sV_{ca}\sqrt{2}(\omega\cos\theta_2 + s\sin\theta_2) - (V_{C\max} - V_v)(s^2+\omega^2)}{2L_l(s^2+\omega^2)\left(s^2 + \frac{2R_l + R_v}{2L_l}\cdot s + \frac{1}{2L_lC}\right)} \tag{8}$$

D. Recharging Mode in a Neutral Grounding 3-phase Power Grid

So far the proposed AC SSCB has been described and designed under the assumption of a non-grounded 3-phase power grid. More importantly, it can also be applied to a neutral grounding 3-phase power grid. For that purpose the proposed AC SSCB does not need to be structurally changed, and the operation characteristics of charging and breaking modes are the same. Fig. 19 shows the recharging loop under the worst condition of a three-phase line-to-ground fault. When the three-phase line-to-ground fault occurs at a power grid, the proposed AC SSCB can quickly break the fault

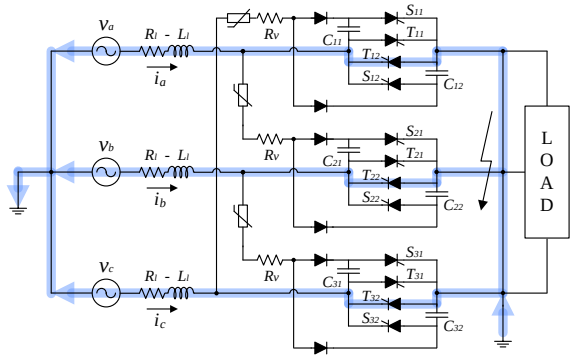

Fig. 19. Recharging loop of AC SSCB in the 3-phase line to ground fault.

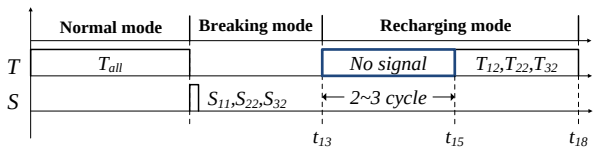

Fig. 20. Triggering method A of Recharging Mode in neutral grounding 3-phase power grid.

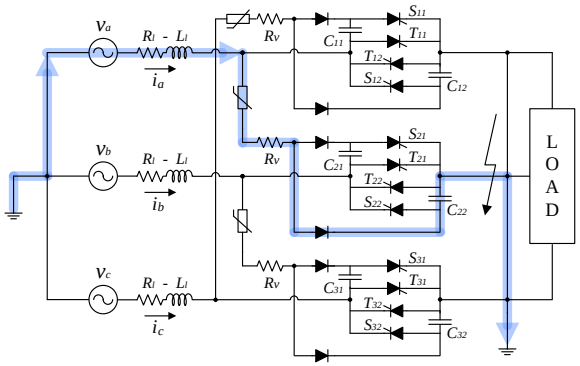

Fig. 21. Recharging loop of C_{22} in the 3-phase ground fault by the triggering method A.

current by using the proposed triggering method shown in Figs. 20 and 22.

(1) Triggering Method A of the Recharging Mode

In the case of a neutral grounding 3-phase power grid, when operating the recharging mode of the SSCB according to the triggering method of Fig. 20, both stable and reliable recharging and rebreaking can be obtained.

Fig. 21 shows the recharging loop of the capacitor C_{22} after the first fault breaking under the line-to-ground fault condition. In the initial stage of the recharging mode, the SSCB has no turn-on signal for 2-3 cycles of the SCR, T_{12}, T_{22}, and T_{32}. The capacitor C_{22} is naturally recharged to the voltage V_a-V_v by the recharging loop of Fig. 21. By this principle, the capacitors C_{12} and C_{32} are also naturally recharged at sections t_{13}-t_{15}. At this time C_{11}, C_{21}, and C_{31} are also naturally recharged.

The recharging voltages of the capacitors C_{12}, C_{22}, and C_{32} are determined as the minimum voltage necessary to break the fault current, which enables the reclosing and rebreaking of the SSCB even under the line-to-ground fault condition.

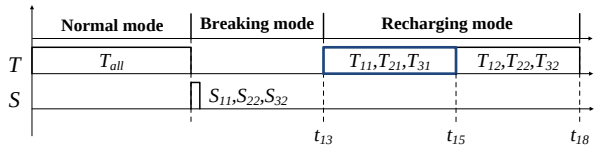

Fig. 22. Triggering method B of Recharging Mode in neutral grounding 3-phase power grid.

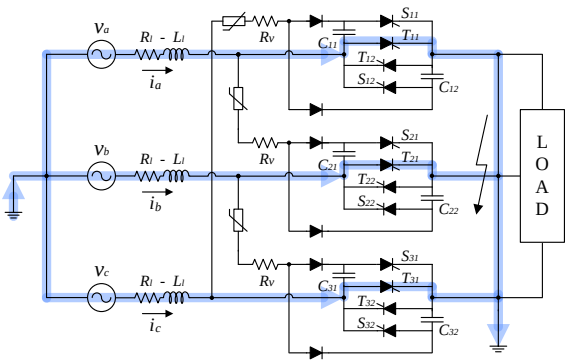

Fig. 23. Recharging loop of C_{22} in the 3-phase ground fault by the triggering method B.

At sections t_{15}-t_{18} of Fig. 20, the proposed AC SSCB turns on the SCR, T_{12}, T_{22}, and T_{32}. If the three-phase line-to-ground fault is not cleared yet, as shown Fig. 19, the proposed SSCB can carry out the rebreaking operation by using the already recharged capacitor at the t_{13}-t_{15} section. In other words, turning on the SCR, T_{12}, T_{22}, and T_{32} at sections t_{15}-t_{18} of the recharging mode is a kind of pre-test procedure for the reclosing operation. If the fault is no longer detected, the original reclosing operation can start.

(2) Triggering Method B of the Recharging Mode

As shown in Fig. 22, this method initially detects whether the line-to-ground fault lasts or not. The load situation can be detected by turning on the SCRs, T_{11}, T_{21}, and T_{31} as shown in Fig. 23. These turn-on operations can be initiated since the capacitors C_{11}, C_{21}, and C_{31} are already naturally recharged regardless of the line-to-ground fault. At this stage, the turn-on operation of the SCRs, T_{11}, T_{21}, and T_{31} is a kind of reclosing operation in the case of a fault situation. After that, if the load side is in the normal state but not in the fault state, the proposed SSCB recharges the capacitors C_{12}, C_{22}, and C_{32} by turning on the SCRs, T_{12}, T_{22}, and T_{32}, which enables the original reclosing and rebreaking operations.

IV. Simulation and Experimental Results

Table II shows the specifications of the prototype designed to implement the proposed AC SSCB shown in Fig. 5. In particular, the operating characteristics of the proposed SSCB are verified under the three-phase short circuit fault condition. The experimental results of each mode are as follows.

A. *Charging Mode* ($t_0 \le t < t_5$)

Fig. 24 shows the simulation waveforms of the three-phase currents i_a, i_b, and i_c and capacitor voltages in the charging

TABLE II
EXPERIMENTAL MODEL PARAMETERS

Parameters	Specification
Power rating	5 [kW]
Varistor	260 [V]
R_V	3 [Ω], 20 [W]
C	100 [uH], 440 [V]
SCR	1200[V], iav=40[A], ipeak= 800[A]
Diode	1200[V], iav=40[A], ipeak= 800[A]

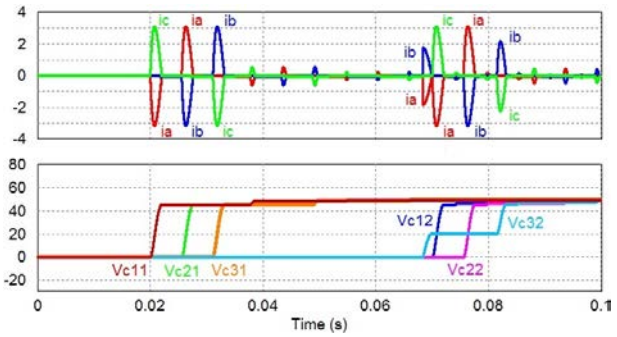

Fig. 24. Current i_a, i_b, i_c and voltage V_{C11}, V_{C12}, V_{C21}, V_{C22}, V_{C31}, V_{C32} simulation waveforms in charging mode.

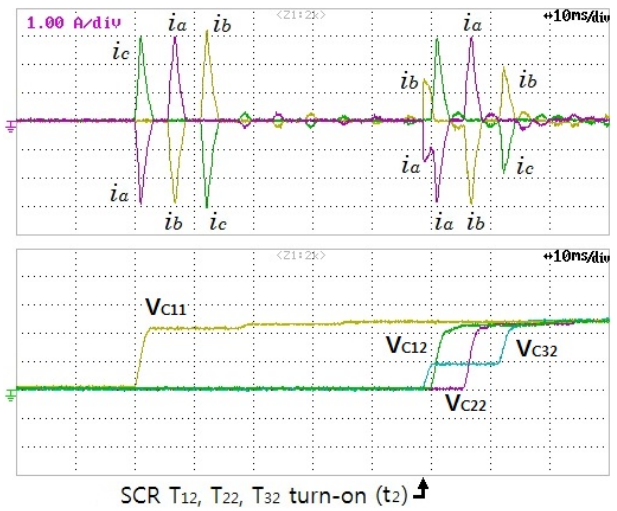

Fig. 25. Measured current i_a, i_b, i_c and voltage V_{C11}, V_{C12}, V_{C22}, V_{C32} waveforms in charging mode.

mode (t_0-t_5). Fig. 25 shows the measured waveforms corresponding to Fig. 24. This confirms that the charging current at the time interval (t_2-t_3) of Fig. 9 flows when turning on the SCRs, T_{12}, T_{22}, and T_{32} at t_2. It also shows that the commutation capacitor voltages are established well enough to interrupt the fault current.

B. Breaking Mode (short circuit fault: $t_7 \le t < t_{13}$)

Fig. 26 shows the simulation waveforms of i_a, i_{Rv}, i_{S11}, and i_{T11} in the breaking mode and their enlarged waveforms. Fig. 27 shows the measured waveforms corresponding to Fig. 26. It shows that the fault current is interrupted rapidly within 400 usec.

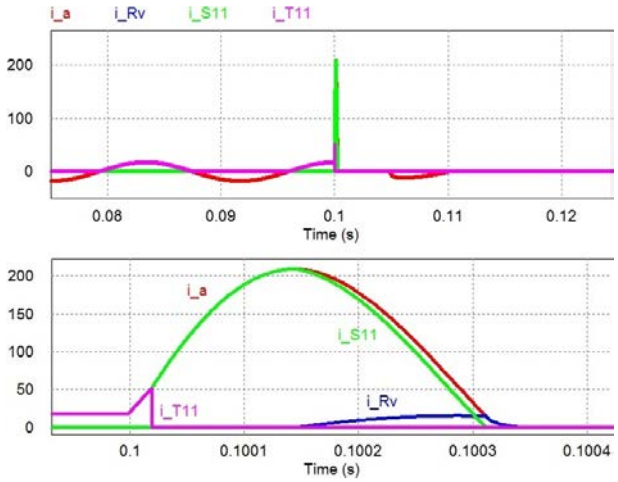

Fig. 26. Current ia, i_{Rv}, i_{T11} and i_{S11} simulation waveforms in breaking mode.

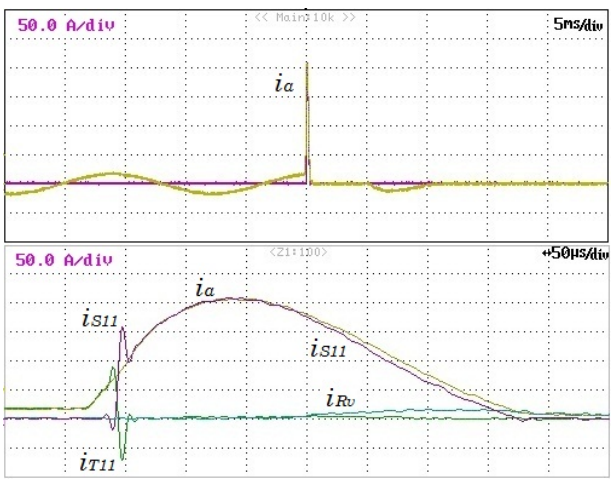

Fig. 27. Measured current i_a, i_{Rv}, i_{T11} and i_{S11} waveforms in breaking mode.

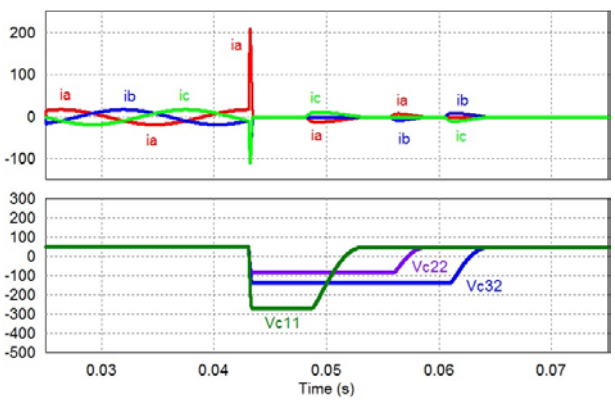

Fig. 28. Current i_a, i_b, i_c and voltage V_{C11}, V_{C22}, V_{C32} simulation waveforms in recharging mode

C. Recharging Mode ($t_{13} \le t < t_{18}$)

Fig. 28 shows the simulation waveforms of the phase current i_a, i_b, and i_c in the recharging mode (t_{13}-t_{18}) and the capacitor voltages V_{C11}, V_{C22}, and V_{C32}. Fig. 29 shows the measured waveforms corresponding to Fig. 28. It shows that the commutation capacitors are recharged well by recharging

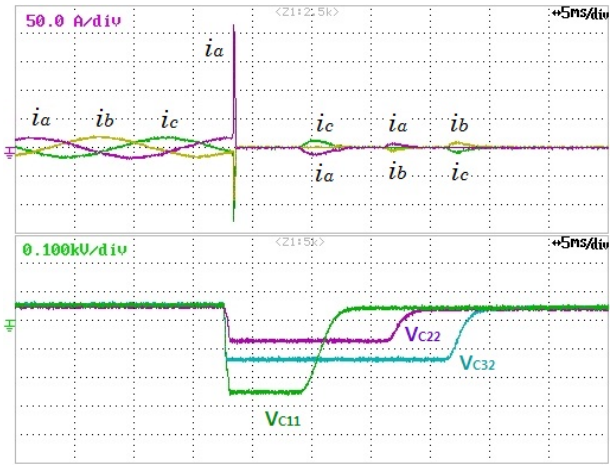

Fig. 29. Measured current i_a, i_b, i_c and voltage V_{C11}, V_{C22}, V_{C32} waveforms in recharging mode.

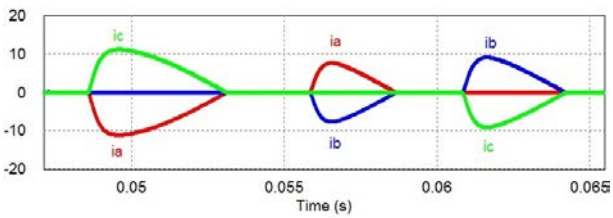

Fig. 30. Phase current i_a, i_b, i_c simulation waveforms in recharging mode.

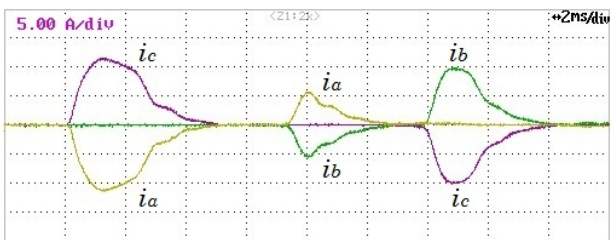

Fig. 31. Measured phase current i_a, i_b, i_c waveforms in recharging mode

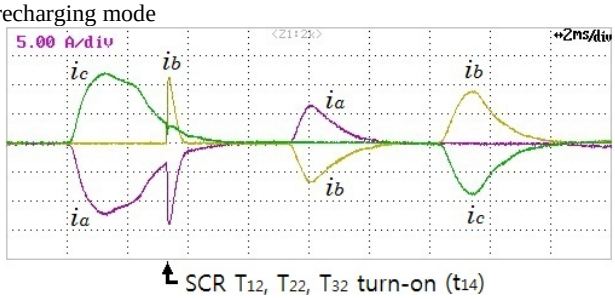

Fig. 32. Measured phase current i_a, i_b, i_c waveforms in recharging mode that include 3-phase short circuit

the loop of Fig. 10 even in the worst state where the three-phase short circuit lasts.

Fig. 30 shows the enlarged simulation waveforms of the three-phase currents i_a, i_b, and i_c in the recharging mode, while Fig. 31 shows the measured waveforms corresponding to Fig. 30. Fig. 32 shows the experimental waveforms of the recharging currents that include the recharging loop of Fig. 11 when turning on SCR T_{12}, SCR T_{22}, and SCR T_{32} at t_{14}.

This shows that a large fault current does not flow even if a charging current that occurs at t_{14} passes through the short circuit. Figures 30, 31, and 32 show that the commutation capacitors are stably recharged even in the worst case where the short circuit condition lasts.

V. CONCLUSIONS

This paper proposes a new AC SSCB that can perform the operating duty of reclosing and rebreaking without a lot of additional devices. Even in the worst case where a short circuit fault lasts, the proposed AC SSCB can charge the commutation capacitor. As a result, it can also perform the operating duty of reclosing and rebreaking regardless of the fault state on the load side. In addition, it is more economical since it reduces the number of varistors and uses low-priced resistors.

Even in a neutral grounding 3-phase power grid, since the proposed AC SSCB can detect line-to-ground faults with a simple control, it can be applied to both neutral floating and neutral-grounding three-phase power systems.

The operating characteristics of the proposed SSCB were verified by simulation and experimental results on three-phase short circuit faults. In addition, this paper suggests design guidelines so that it can be applied to a lot of applications. It is anticipated that the proposed AC SSCB will be widely utilized to realize the power schemes of high power quality systems.

ACKNOWLEDGMENT

This work was supported by the Pukyong National University Research Abroad Fund in 2011(PS-2011- 011).

REFERENCES

[1] C.-N. Lu and C.-C. Shen, “Estimation of sensitive equipment disruptions due to voltage sags,” *IEEE Trans. Power Del.*, Vol. 22, No. 2, pp. 1132-1137, Apr. 2007.

[2] N. Hatziargyriou, H. Asano, R. Iravani, and C. Marnay, “Microgrids,” *IEEE Power Energy Mag.*, Vol. 5, No. 4, pp. 78-94, Jul./Aug. 2007.

[3] F. Katiraei and M. R. Iravani, “Power management strategies for a microgrid with multiple distributed generation units,” *IEEE Trans. Power Syst.*, Vol. 21, No. 4, pp. 1821-1831, Nov. 2006.

[4] G. Parise and L. Parise, “Unprotected faults of electrical and extension cords in AC and DC systems,” *IEEE Trans. Ind. Appl.*, Vol. 50, No. 1, pp.4-9, Jan. 2014.

[5] C. Abbey, D. Cornforth, N. Hatziargyriou, K. Hirose, A. Kwasinski, E. Kyriakides, G. Platt, L. Reyes, and S. Suryanarayanan, “Powering through the storm: Microgrids operation for more efficient disaster recovery,” *IEEE Power Energy Mag.*, Vol. 12, No. 3, pp. 67-76, May/Jun. 2014.

[6] C37.09, IEEE Standard Test Procedure for AC High-Voltage Circuit Breakers Rated on a Symmetrical Current Basis, IEEE Std C37.013-1993, 2000.

[7] S. Lee and H. Kim, "A study on low-voltage DC circuit breakers," *IEEE International Industrial Electronics Symposium on Industrial Electronics (ISIE)*, pp. 1-6, 2013.
[8] J.-Y. Kim, I.-D. Kim, and E.-C. Nho, "A novel DC solid-state circuit breaker for DC grid," *Transactions of Korean Institute of Power Electronics(KIPE)*, Vol. 17, No. 4, pp. 368-376, Aug. 2012.
[9] C. Meyer, S. Schroder, and R. W. De Doncker, "Solid-State circuit breakers and current limiters for medium-voltage systems having distributed power systems," *IEEE Trans. Power Electron*., Vol. 19, No. 5, pp. 1333-1340, Sep. 2004.
[10] C. Meyer and R. W. De Doncker, "Solid-state circuit breaker based on active Thyristor topologies," *IEEE Trans. Power Electron*., Vol. 21, No. 2, pp. 450-458, Mar. 2006

Jin-Young Kim received his B.S. degree in Electrical Engineering from Pukyong National University, Busan, Korea, in 2004, his M.S. degree in Electrical Engineering from Pusan National University, Busan, Korea, in 2006, and his Ph.D. degree in Electrical Engineering from Pukyong National University, Busan, Korea, in 2014. His current research interests include solid-state circuit breakers and their applications.

Seung-Soo Choi was born in Busan, Korea, in 1982. He received his B.S. and M.S. degrees in Electrical Engineering from Pukyong National University, Busan, Korea, in 2013 and 2015, respectively, where he is presently working towards his Ph.D. degree. His current research interests include power electric control, power converters and power amplifiers.

In-Dong Kim received his B.S. degree in Electrical Engineering from Seoul National University, Seoul, Korea, in 1984, and his M.S. and Ph.D. degrees in Electrical and Electronic Engineering from the Korea Advanced Institute of Science and Technology (KAIST), Daejeon, Korea, in 1987 and 1991, respectively. From 1991 to 1996, he was a Principal Engineer at the Rolling Stock R&D Center of Daewoo Heavy Industries, Ltd., Korea. From 1997 to 1998, he did Post-Doctoral research in the Department of Electrical and Computer Engineering, University of Tennessee, Knoxville, TN, USA. From 2004 to 2005, he served as a Visiting Professor in the Bradley Department of Electrical Engineering, Virginia Tech, Blacksburg, VA, USA. From 2012 to 2013, he served as a Visiting Professor at the FREEDM Systems Center, North Carolina State University, Raleigh, NC, USA. He has been a Senior Member of the IEEE since February 2007. In 1996, he joined the Department of Electrical Engineering, Pukyong National University, Busan, Korea, where he is presently a full Professor. His current research interests include power electronics, motor drives, power quality control, renewable distributed power sources, and DSP-based control of power converters.